J Fluoresc (2012) 22:1383–1393
DOI 10.1007/s10895-012-1077-6

ORIGINAL PAPER

Novel Quadruple Fluorescence Properties of Two Benzoylthiourea Isomers

Wen Yang · Wei Zhu · Weiqun Zhou · Huanhuan Liu · Yunlong Xu · Jianfen Fan

Received: 20 December 2011 / Accepted: 11 June 2012 / Published online: 19 June 2012

Abstract Two benzoylthiourea isomers, N-2-flurobenzoy-N'-4- (N,N-dimethyl)amidophenylthiourea (2FBDAPT) and N-4-fluro-benzoy-N'-4- (N,N-dimethyl)amidophenylthiourea (4FBDAPT) were determined by fourier transform infrared spectroscopy (FTIR), nuclear magnetic resonance (NMR) and X-ray diffraction. It was found that intra- and intermolecular hydrogen bonds played an important role in determining their conformations. Electronic spectra of the two compounds were investigated by UV absorption and steady-state fluorescence methods. The intermolecular hydrogen bond between the title compounds and methanol molecules caused the long wavelength absorption bands in methanol to weaken and vanish indeed. Quadruple fluorescence bands in ultraviolet and visible region were observed in the studied solvents upon the variable excitation wavelength. As same as Azumaya's suggestions for benzanilide (BA), F4 fluorescence bands with the maximum wavelength (λ_{max}) between 546 nm and 622 nm were characteristic of TICT fluorescence. F3 bands of λ_{max} from 434 nm to 483 nm were explained by the ESIPT model of the S1 state of the thiol tautomer to the S1 state of the keto tautomer. The new proposition was that F2 bands with λ_{max} at about 365 nm were attributed to ESIPT from the S1 state of the thiol tautomer to the S0 state of the enol tautomer. And F1 fluorescence emissions with λ_{max} at about 310 nm originated from the local S1 transitions of the enol tautomer. All experimental results were supported by MP2, CASSCF and CASPT2 quantum chemical calculations.

W. Yang · W. Zhu · W. Zhou (✉) · H. Liu · Y. Xu · J. Fan
College of Chemistry, Chemical Engineering and Materials Science, Soochow University,
199 Ren'ai Road,
Suzhou 215123, People's Republic of China
e-mail: wqzhou@suda.edu.cn

Keywords Benzoylthiourea isomers · Electronic spectra · Fluorescence property · Quantum chemical calculations

Introduction

Sulfamide and thiourea have been extremely studied due to the applications in the field of supramolecular chemistry [1–8] as 'host' molecules for recognition of 'guest' anions. Sulfamide and thiourea moieties have become the focus of the development of neutral anion receptor, because the hydrogen bonding of these functional groups is directional in character, resulting in relatively strong complexes with various anions [9–15].

The double fluorescence of BA has been observed by previous workers [16–22]. The local emissions of weak short wave fluorescence and the high wave emissions in polar solvent show the characteristics of the n-π* state and the ICT (intra-molecular charge transfer) state. So far, two main models are used to discuss the long wavelength fluorescence emission of BA. The PT (proton transfer)/ICT model was proposed by Kasha et al. [16–18]. The twisted intra-molecular charge transfer (TICT) was proposed by Azumaya et al. [19]. Further, excited state intramolecular proton transfer mechanism (ESIPT) of the imine tautomer of these compounds was suggested by Lewis et al. [22]. We have observed infrared absorption of the group -C=N- in FTIR spectrum of N-2-fluorobenzoyl-N'-4-methoxyl phenylthiourea (FBMPT) as the analog [23]. Double fluorescence bands of FBMPT have been detected in polar solvents. It revealed that the short wavelength fluorescence derived from deactivation of local excited state and the large Stokes shift fluorescence was resulted from ESIPT or TICT. However, it hasn't been clear which intramolecular charge transfer (ICT) the large Stokes shift fluorescence belongs to, TICT or ESIPT model.

The existence of TICT states has often been invoked to interpret the photophysical properties of fluorophores, especially those possessing an anilino moiety. In the present work, the donor-acceptor molecular model of N-benzoylthiourea was designed. Taking dimethylamino as donor and fluorine as acceptor, both FBDAPTs were prepared and structurally and photo-physically characterized. Herein, with the aid of quantum chemical calculations, we attempt to understand the luminescence mechanism to provide guidance for future searches for new fluorescent materials and further explorations of their applications.

Experimental and Theoretical Methods

Synthesis and Measurement Method

In order to explore the effect of the intramolecular hydrogen bonds, fluorine atom was added to the benzoyls as an acceptor (A). And 4-N,N-dimethylaminoanilino was connected to thiocarbonyl as a donor (D). The designed two D-A molecules are shown in Scheme 1. 2FBDAPT formed two intramolecular hydrogen bonds of N-H...O and N-H...F, and 4FBDAPT formed one intramolecular hydrogen bond of N-H...O.

The title compounds were synthesized and purified as described previously [23]. FTIR spectra were obtained from KBr discs using a Nicolet 170SX FT-IR spectrometer. The NMR spectrum was recorded in $CDCl_3$ as solvent, at room temperature and at 400 MHz on an INOVA 400 instrument. The crystal structures were determined using X-ray diffraction with a MERCURY CCD detector. The data were corrected for Lorentz and polarization effects. The structures were solved using direct methods [24] and expanded using Fourier techniques [25]. The absorption spectra were recorded on a CARY50 UV–VIS spectrophotometer. The absorption spectra have been determined in the studied solvents at the concentration of 2×10^{-5} mol·L^{-1}. The fluorescence measurements were carried out using an FLS920 analytical instrument. The fluorescence spectra have been determined in the concentration of 1×10^{-4} mol·L^{-1} and 1×10^{-5} mol·L^{-1} respectively. The fluorescence quantum yield (QY) was detected with quinine sulfate in 0.05 mol·L^{-1} sulfuric acid and 2-aminopyridine in 0.1 N H_2SO_4 as the standard. Organic solvents were purified by distilling and have been checked to show no fluorescent impurity.

Method of Calculation

We have performed electronic structure calculations to explore possible photophysical mechanisms. As a starting point, the geometry optimization were performed by employing Becke's three-parameter hybrid method (B3LYP) [26–28] with a Pople basis set, 6–31 G(d) using the program package *G03* [29]. The harmonic vibration frequencies were calculated to confirm the stable structures. Subsequently, the ground-state minima structures have been obtained by MP2 [30] method at the same level. The complete active space self-consistent field (CASSCF) methods [31, 32] with an active space consisting of 12 electrons in ten orbits were used to explore the excited state electronic structures. Pople basis set, 6–31 G(d) was used in all subsequent steps. For each optimized structure, we have performed single-point CASPT2 calculations [33, 34]. All of the CASSCF and CASPT2 calculations were performed with the MOLPRO electronic code package [35, 36].

Results and Discussion

Crystal Structures

The triclinic crystal structure of 2FBDAPT belongs to the space group: *P-1*, a=8.859(3)Å, b=9.872(4)Å, c=10.232(4)Å; α=113.401(6)°, β=92.778(4)°, γ=108.351(4)°; V=763.8(5)Å^3, Z=2; d_{calc}=1.380 mg/m^3, F(000)=332, R_{int}=0.0323. Whereas the monoclinic crystal structure of 4FBDAPT, belongs to the space group: *P21/c*, a=11.348(5)Å, b=11.245(5)Å, c=12.059(5)Å; β=97.247(19)°; V=1526.5(11)Å^3, Z=4; d_{calc}=1.381 mg/m^3, F(000)=664, R_{int}=0.1213. The structures were deposited in the Cambridge Crystallographic Data Center (CCDC 832390 and 832391). The crystal structures and crystal packing of the FBDAPTs are shown in Fig. 1.

For the crystal of 2FBDAPT, there were two intramolecular hydrogen bond interactions, the hydrogen bond of N(1)-H(1)···F(1), with the following parameters; the distance of N(1)···F(1), 2.685 Å, the distance of H(1)···F(1), 1.96 Å, the angle of N(1)-H(1)···F(1), 140.3 °; the hydrogen bond of N(2)-H(2)···O(1), the distance of N(2)···O(1), 2.667 Å, the distance of H(2)···O(1), 1.98 Å, and the angle

Scheme 1 The structures of two benzoylthiourea derivatives in this study

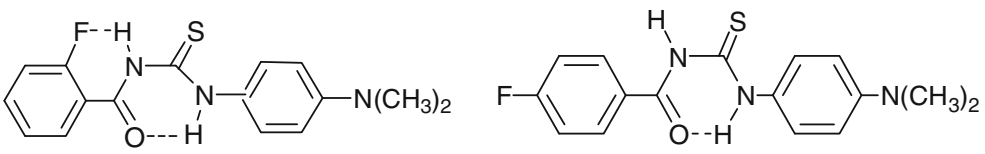

2FBDAPT 4FBDAPT

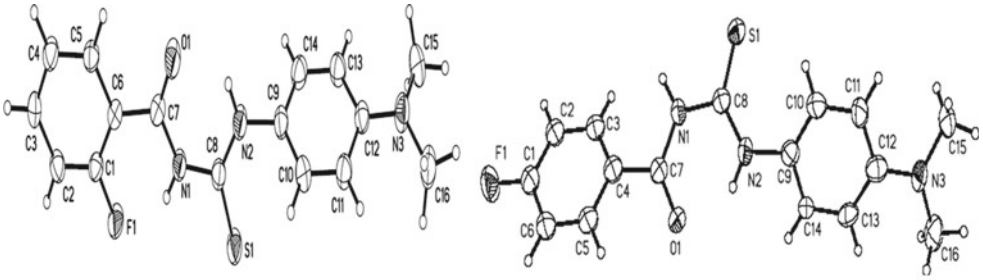

Fig. 1 The crystal structures and crystal packing of the FBDAPTs

The structures by X-ray, ellipsoids were plotted at the 40% probability

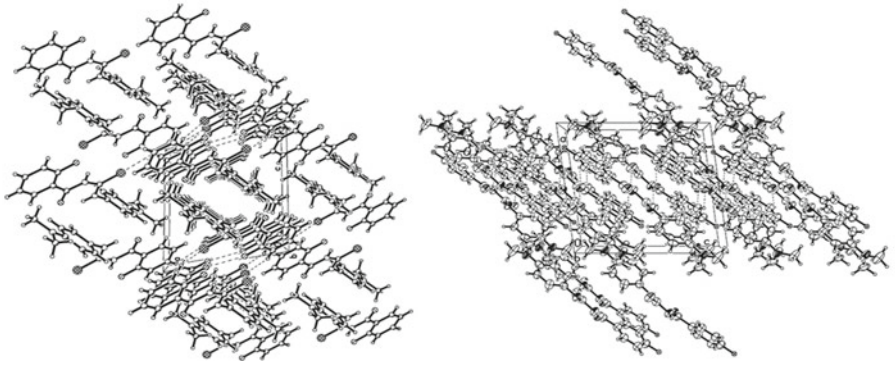

The crystal of packing by an axis b

2FBDAPT

The crystal of packing by an axis b

4FBDAPT

of N(2)-H(2)···O(1), 134.8 °. Whereas in the molecule of 4FBDAPT crystal, only one intra-molecular hydrogen bond, N(2)-H(2A)···O(1) was found, the distance between N(2) and O(1) was 2.628 Å, and the distance between H(2A) and O(1) was 1.91 Å, with an angle of 139.3 °.

NMR and FTIR

^{1}H NMR ($CDCl_3$): 2FBDAPT, δ=2.98 (s, 6H, $N(CH_3)_2$), 6.741 (d, J=8.4Hz, 2H, C13-H, C11-H), 7.235 (q, $J_{2,3}$= 8.0Hz, $J_{F,H}$=4.0Hz, $J_{3,4}$=8.4Hz, 1H, C3-H), 7.356 (t, $J_{3,4}$= $J_{4,5}$=8.0Hz, 1H, C4-H), 7.513 (d, J=9.6Hz, 2H, C10-H and C14-H), 7.654~7.594 (m, 1H, C2-H), 8.093 (t, $J_{4,5}$=8.0Hz, $J_{5,\ N(2)H}$=8.0Hz, 1H, C5-H), 9.604 (br, s, 1H, N2-H), 9.640 (br, s, 1H, N1-H) ppm. 4FBDAPT δ=2.981 (s, 6H, $N(CH_3)_2$), 6.750 (d, J=8.8Hz, 2H, C13-H, C11-H), 7.219 (t, $J_{5,6}$=8.4Hz, $J_{3,4}$=8.8Hz, 2H, C3-H, C5-H), 7.495 (d, J= 8.8Hz, 2H, C10-H and C14-H), 7.922 (q, 2H, $J_{5,6}$=$J_{2,3}$= 5.2Hz, $J_{F,H}$=3.6Hz, 2H, C2-H, C6-H), 9.042 (br, s, 1H, N2-H) ppm.

The measured infrared spectra of the title compounds shows that ν(C=O) and ν(C=S) have already shifted to lower frequencies while the ν(NCN) have shifted to higher frequencies, due to the π conjugation. Both peaks at 3426 cm^{-1} correspond to the stretching ν(N1-H1) vibrations. The decrease of the absorption of 2FBDAPT molecule indicated to the existence of the intramolecular hydrogen bond. The bands at 3226 cm^{-1} attributed to the ν(N2-H2) reveals the existence of an intra-molecular hydrogen bond. The peaks assigned to ν(Ph-H) are sheltered in the wide band at 3071 cm^{-1} and 3035 cm^{-1}. The bands at 2881 cm^{-1} and 2805 cm^{-1} are assigned to the asymmetric and symmetric ν(CH_3) stretching vibrations, respectively. The weakly bands at 2365 and 2339 cm^{-1} should be assigned to the stretching vibration of ν(S-H), which indicates the existence of the thiol tautomers. The strong absorbing ν(C=O) band, which appears at 1676 cm^{-1} and 1669 cm^{-1} apparently decreases in frequency relative to the ordinary carbonyl absorption (1710 cm^{-1}) due to conjugated resonance with the phenyl ring and by the formation of intra-molecular hydrogen bonding with N-H. The bands at about 1614 cm^{-1} are attributed to the vibration of the phenyl ring. The abnormally intense absorption peak at 1523 cm^{-1} is regarded as the asymmetric stretching vibrations of N-C-N. It reveals that intra-molecular hydrogen bonding exists in the compound. The intense absorption bands at 1518, 1513 cm^{-1} indicate the presence of C=N double bonds. The stretching vibration of C=S bonds appears at about 1278 cm^{-1}.

Ultraviolet Visible Spectra

We compared and critically analyzed the absorption and fluorescence characteristics in four different solvents, namely 1,4-dioxane (an aprotic solvent of low polarity, ε=2.21), THF (an aprotic polar solvent, ε=7.58), acetonitrile (an aprotic strong polar solvent, ε=36.64) and methanol (a protic strong polar solvent, ε=32.63). Because title compounds have very low solubility in nonpolar solvents such

as cyclohexane (static dielectric constant, ε_0~2.02), the fluorescence or transient absorption could not be studied in this solvent. We chose 1,4-dioxane (ε_0~2.21) as the representative nonpolar aprotic solvent. The absorption spectra in the studied solvents are depicted in Fig. 2. The maxima absorption wavelengths are listed in Table 1.

As shown in Fig. 2, two isomers exhibit similar absorption characteristics. The absorption bands exhibit the vibrational structures with at least two bands at about 360 nm and 300 nm. From the data of Table 1, there is no significant solvatochromic shift of the absorption maxima as a function of the solvent polarity. Taking 4FBDAPT as an example, the maxima wavelengths, λ_{a1}, of the first absorption bands are at 361 nm in 1,4-dioxane, 360 nm in THF and 358 nm in acetonitrile. The maxima wavelengths, λ_{a2}, of the second absorption bands are at 298 nm in 1,4-dioxane, 300 nm in THF, 297 nm in acetonitrile and 298 nm in methanol. The attenuation of the long wave absorption bands in methanol solvent for both compounds is observed, which is attributed to the intermolecular hydrogen bond interaction between the compounds and methanol molecules.

Fluorescence Property

The fluorescence spectra by the concentration of 1×10^{-4} mol·L^{-1} were recorded. Both compounds exhibit fairly complicated fluorescence emissions. The fluorescence spectra of the title compounds are different from previous determined FBMPT [23]. Generally, both compounds emit the lower energy fluorescence than that of FBMPT and BA. The QY of 4FBDAPT with one hydrogen bond is 10–20 times as intense as that of 2FBDAPT with two hydrogen bonds.

Fluorescence emission spectra of 2FBDAPT in the studied solvents are shown in Fig. 3. The excitation wavelengths are in parentheses. The λ_{max} of the fluorescence bands and the QY are compiled in Table 2. Fluorescence spectra exhibit the fluorescence intensity decreasing with the polarity of the solvents increasing. In the weak polar solvent, 1,4-dioxane, the variable λ_{max} of the wide single fluorescence band changing from 515 nm to 480 nm is observed when the excitation wavelength changes from 388 nm to 330 nm. And the BHW (band half width) increases from 6324 cm^{-1} to 9745 cm^{-1}. Excited at 260 nm, a single fluorescence band with the λ_{max} of 312 nm is observed, which is similar to the emission band of BA [22]. In the polar solvent, THF (ε= 7.58), using the excitation wavelength of 434 nm, the fluorescence spectra display one emission peak with the λ_{max} at 578 nm. When the excitation wavelength reduces to 324 nm, double fluorescence bands are observed. And the long wavelength fluorescence also appears at 578 nm, but the intensity decreases. The λ_{max} of the blue side fluorescence band is at 447 nm. At UV region, no fluorescence emission is detected in THF. In the strong polar aprotic solvent of acetonitrile, excited at 348 nm, the double fluorescence bands are also detected. Comparing that in THF, the double fluorescence bands shift red with the different size and the fluorescence intensity weaken. The λ_{max} of the long wavelength fluorescence shifts red to 622 nm, whereas the λ_{max} of the short wavelength fluorescence shifts red to 459 nm. In the strong polar protic solvent of methanol, only a wide emission band is observed in fluorescent curves. The λ_{max} appears at 434 nm with the excitation wavelength at 331 nm. The abnormal blue shift can be attributed to the intermolecular hydrogen bond interactions between the sample molecules and solvent methanol molecules.

The fluorescence spectra of 4FBDAPT present more complication. Because of the stronger fluorescence than that of 2FBDAPT, the variable wavelength emission upon the excitation wavelength is very obvious. The λ_{max} of the fluorescence bands and QY in the studied solvents are compiled in Table 3. Gradually increasing excitation wavelength from 404 nm to 260 nm, the fluorescence spectra in 1,4-dioxane are exhibited in Fig. 4. At first, we observe a wide fluorescence band with the λ_{max} of 520 nm upon the excitation wavelength of 404 nm. The BHW of the fluorescence band is 7480 cm^{-1}. The λ_{max} of the wide fluorescence

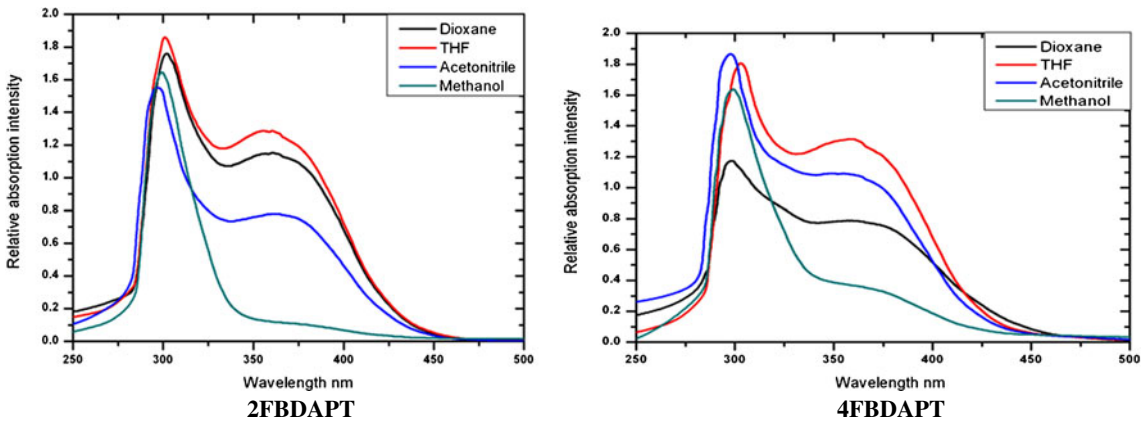

Fig. 2 UV visible absorption spectra of both FBDAPTs in four solvents

Table 1 Maxima absorption wavelengths of both FBDAPTs in the studied solvents

	Solvent	λ_{a1} (nm)	λ_{a2} (nm)
4FBDAPT	Dioxane	361	298
	THF	360	300
	Acetonitrile	358	297
	Methanol		298
2FBDAPT	Dioxane	360	302
	THF	359	303
	Acetonitrile	362	298
	Methanol		300

band shifts to 464 nm upon the excitation wavelength of 370 nm. Increasing the excitation energy to 326 nm, the fluorescence curves show the double undivided well peaks fluorescence with the λ_{max} at 459 nm and 546 nm. Excited at 310 nm, one normal emission peak with the λ_{max} of 361 nm is obtained. Adding the excitation energy to 290 nm, the double fluorescence bands are detected again. Both λ_{max} are at 361 nm and 479 nm. The last, excited at 260 nm, only one fluorescence emission with the λ_{max} of 312 nm in UV region is obtained. Additionally, we observe the λ_{max} change from 464 nm to 485 nm and 492 nm upon the excitation wavelength of 370, 369 and 368 nm. Excitation at progressively shorter wavelengths results in a progressively increase of the fluorescence wavelength, which is similar to the characteristic of BA [22].

The fluorescence spectra of 4FBDAPT in the other solvents are displayed in Fig. 5. In the polar solvent of THF, similar to 2FBDAPT, excited at 354 nm, the fluorescence spectra display double fluorescence bands with the λ_{max} of 584 nm and 472 nm. When the excitation wavelength is reduced to 321 nm, the fluorescence band with the λ_{max} at

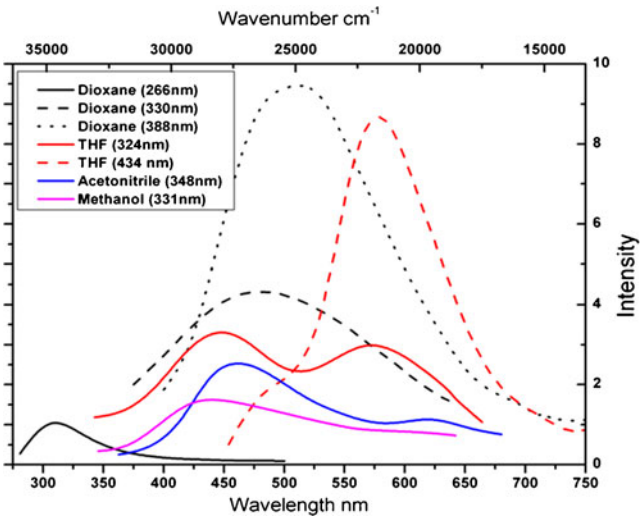

Fig. 3 Fluorescent spectra of 2FBDAPT in the studied solvents

Table 2 The maximum emission, λ_f (nm) and fluorescence quantum yield ($QY \times 10^{-3}$) of 2FBDAPT (excitation wavelengths are in parentheses)

	Dioxane	THF	Acetonitrile	Methanol
λ_{f1}(nm)	312(266)			
QY	0.024			
$\lambda_{f2,3}$(nm)	480(330)	447(324), 578(324)	459(348), 622(348)	434(331)
QY	0.08	0.067, 0.06	0.046, 0.023	0.032
λ_{f3}(nm)	515(388)	578(434)		
QY	0.18	0.16		

578 nm disappeared and the blue side fluorescence band with the λ_{max} of 492 nm increased. When the excitation wavelength is reduced to 260 nm, different from that in 1,4-dioxane, the double peaks are obtained again. Both λ_{max} of the double peaks are at 332 nm and 458 nm. In acetonitrile, the double fluorescence bands shift blue slightly with the different size. The λ_{max} of the red side fluorescence shifts to 550 nm and the fluorescence intensity weakens. And the λ_{max} of the blue side fluorescence shifts to 463 nm and the fluorescence intensity increases. Excited at 308 nm, the red side fluorescence vanishes and the λ_{max} of the blue side fluorescence shifts continuously to 431 nm. In methanol, only a broad fluorescence band appears in fluorescence curves with the maximum wavelength of 434 nm upon the excitation wavelength of 335 nm. Because of the two weak fluorescence emissions of 2FBDAPT upon the excitation wavelength of 260 nm in 1,4-dioxane, we can't observe the fluorescence emission in the other more polar solvents. However, the fluorescence emission band of 4FBDAPT upon the excitation wavelength of 260 nm in 1,4-dioxane is 24 times as intense as that of 2FBDAPT. In the other more polar solvents, the fluorescence emissions are always detected and the fluorescence intensity reduces as the polarity of the solvents enhances. In acetonitrile, we also observe the tail emission at 368 nm.

As shown in the fluorescence spectra, we can divide the fluorescence spectra into four fluorescence bands: F1 fluorescence of the λ_{max} at about 310 nm, F2 fluorescence of the λ_{max} at about 365 nm, F3 fluorescence, the λ_{max} from 434–483 nm and F4 fluorescence of the λ_{max} above 546 nm. For the better interpretation of our experimental results, the excited states of the compounds considered are studied by CASSCF and CASPT2 methods. Differences in fluorescence spectra in various solvents are discussed in detail.

Quantum Chemical Calculation

Quantum chemical calculation is based on the example of 4FBDAPT. The compounds have the hexatomic ringed structure by the formation of the intramolecular hydrogen bond of N-H...O [24]. The existence of the hydrogen bond should incumber the rotation about the benzamide C-N bond

Table 3 The maximum emission, λ_f (nm) and fluorescence quantum yield (QY×10^{-3}) of 4FBDAPT (λ_e(nm) is excitation wavelength)

Solvents	Dioxane	QY	THF	QY	Acetonitrile	QY	Methanol	QY
λ_e(nm)	260		260		258		267	
λ_f (nm)	311	0.48	332, 458	0.12, 0.20	309, 368	0.28, 0.12	307	0.21
λ_e(nm)	310		321		308		335	
λ_f (nm)	361	0.45	492	0.19	431	0.12	450	0.092
λ_e (nm)	290							
λ_f (nm)	364, 479	0.15, 0.26						
λ_e(nm)	326		354		332			
λ_f(nm)	459, 546	0.21, 0.23	472, 584	0.10, 0.075	463, 550	0.15, 0.085		
λ_e(nm)	370							
λ_f(nm)	464	0.55						
λ_e(nm)	404							
λ_f (nm)	520	0.3						

similar to BA[22]. A PES (Potential Energy Scan) is carried out by rotating about the C-N bond of aniline. The structures for the rotational coordinates are optimized with respect to all coordinates except for the torsion angle defined by the atoms C (8)-N (2)-C (9)-C (10) (Fig. 1). Two minima in potential energy curve are fully optimized without constraints. The structure for each point is confirmed by vibration analysis, indicating no imaginary frequencies. Based on MP2 calculations of the ground state, we optimize the structures of the first excited state using CASSCF method. And single point energy is calculated by CASSPT2 method for each optimized structure of the excited state. The potential energy curve of the ground state by CASPT2 method is shown in Fig. 6.

Two minima structures are found in the potential energy curve of the ground state. The one was located at 37.5 ° and the other at 138.4 ° is slightly higher in energy by 0.01 eV. The rotational barriers for both conformers are defined by the peaks at 90 °, where the barrier is calculated to be 0.68 eV (72.3 kJ/mol). The energy difference for the S0 and S1 states of both minima conformers are calculated to be 4.42 eV and 4.60 eV. As a consequence, the conformer at 138.4 ° in the excited state is less stable by 0.18 eV compared to the conformer at 37.5 °. The energy gap for the S0 and S1 states for the conformer at 90 ° is calculated to be 1.72 eV.

As we know, the enol and thiol of these compounds can exist stably by the intramolecular proton transfer respectively. ^{1}H NMR and FTIR methods have detected the chemical shift of the proton of enol and the stretching vibration frequency of sulfhydryl group, which illuminates the existence of the thiol and enol tautomers. Both of enol and thiol tautomers of the ground state are optimized at the level of MP2/6–31 G(d). The structures of the excited singlet states for two rotating isomers (keto isomers) and two tautomers (enol and thiol) are optimized by CASSCF methods. The structures of the ground states and the excited states are displayed in Fig. 7. 4FBDAPT in the ground state is composed of three parts, benzoyl ring, the carbonylthiourea ring, which is composed by an intra-molecular hydrogen bond between the carbonyl and the amido of thiourea, and the toluidine plane. There is an angle between the benzoyl ring and the carbonylthiourea ring with 29.5 °. Dihedral angle of carbonylthiourea and toluidine is 37.9 °. For the structure of

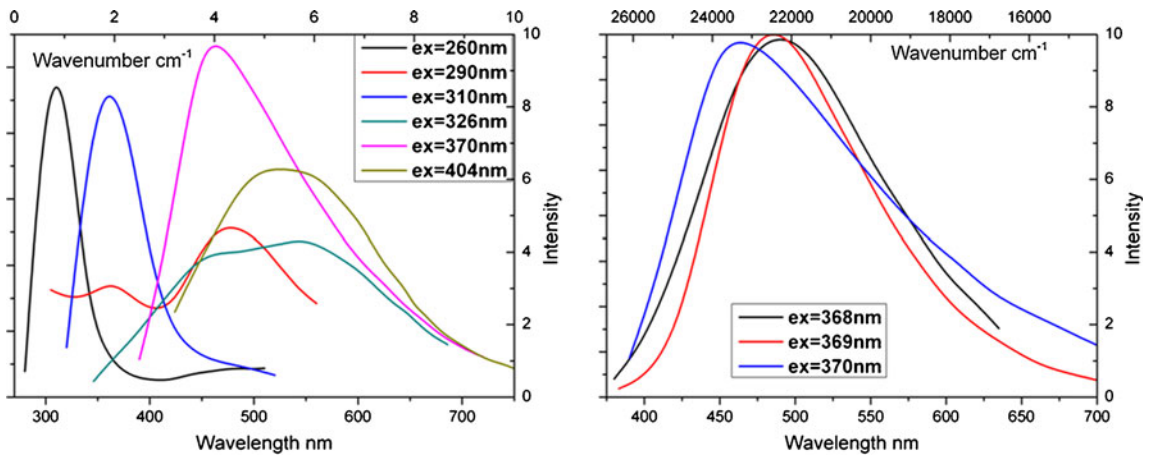

Fig. 4 Fluorescence spectra of 4FBDAPT in 1,4-dioxane

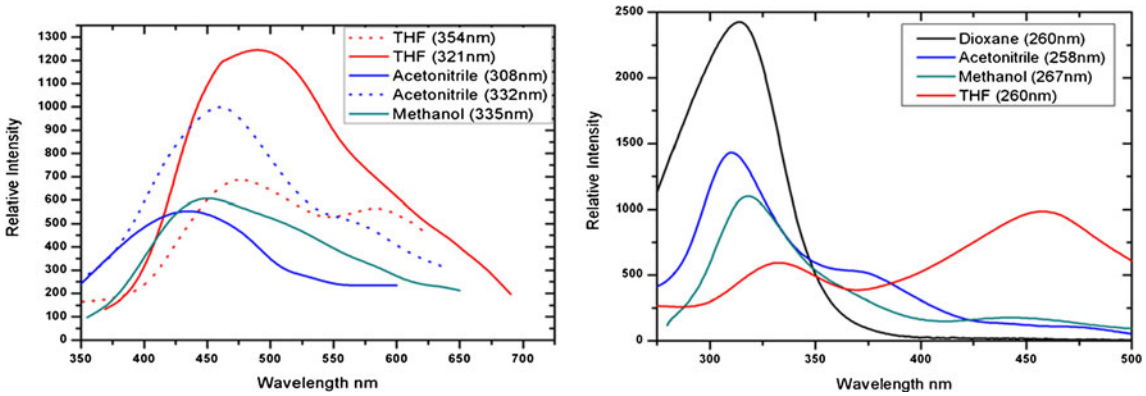

Fig. 5 Fluorescence spectra of 4FBDAPT in the solvents except for 1,4-dioxane

the first excited states, both C-N bond lengths are at average. The double bond, C=S (1.655 Å), become the single bond (1.756 Å). The bond C=O is shortened from 1.24 Å to 1.2 Å, which indicates the conjugation decrease. The structures of both rotating isomers in the first excited state are very different from that in the ground state. The molecular structures are extremely twisted in the first excited state. As noted by Kasha and co-workers [18], the large Stokes shift for fluorescence bands is indicative of a large change in geometry prior to fluorescence. There is little change of the structures between the first excited states and the ground-state for both enol and thiol tautomers, which shows the local excited (LE) characteristic of the first excited state. CASPT2 calculated energy levels are shown in Fig. 8. Similar to the common thiocarbonyl compounds [37, 38], both keto isomers have the low energy level of the first excited state.

In general, three mechanisms may be considered as the origin for the multi- fluorescence bands. (a) The compound exists in the different conformations in the ground and excited state. These conformations have different energies and are separated by a significant energy barrier. Thus, the different emission rates are the result of equilibrating conformers with different fluorescence lifetimes. (b) Upon irradiation, the different transitions take place and lead to the independent excited states. The excited states are deactivated by fluorescence, however, with significantly different emission rates. (c) The excited state intramolecular charge transfer states can be existed. In the excited state, an intramolecular charge transfer may emit at different wavelengths and with different fluorescence lifetimes.

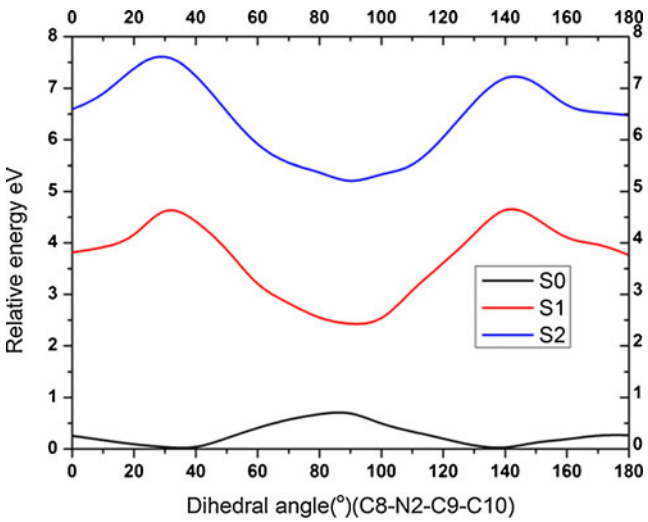

Fig. 6 Calculated potential energy surfaces of the first excited singlet state structure for amide C-N rotation in 4FBDAPT (0 ° is *Z* isomer and 180 ° is *E* isomer) by CASPT2 method

Two minima conformations in the ground state of 4FBDAPT have almost the same energy levels. The low energy barrier between both conformations in the ground state (0.68 eV) indicating the different emission rates shouldn't be the result of equilibrating conformers with different fluorescence lifetimes.

According to Kasha's opinion of BA, we explain the F4 emission band as the TICT model. Large Stokes shift is the character of TICT fluorescence. The maximum Stokes shifts of F4 are 274 nm for 2FBDAPT and 230 nm for 4FBDAPT in acetonitrile respectively. Additionally, the Stokes shifts of F4 increase as the polarity of the solvents increase. Taking 4FBDAPT as an example, the Stokes shift increases from 220 nm in 1,4-dioxane to 230 nm in THF. And the intensity of F4 decreases with the increase of the solvent polarity. The TICT model has been presented since the discovery of the dual fluorescence of p-dimethylaminobenzonitrile by Lippert et al. [39]. A TICT state needs the full or nearly full formation of electron transfer between donator and acceptor group the twisted configuration against each other by 90 ° [40]. As shown in Fig. 8, because of the large structural twist in the first excited state, the transition of S1/S0 can be assigned to twisted intramolecular charge transfer (TICT) transition. According to the calculation in Fig. 9, the energy gap between S0 and S1 is 2.4 eV. Comparing with the maximum wavelength of the fluorescence band of experiments, 2.12 eV (584 nm) in THF, the error is 0.28 eV. The result of PES can also check this assumption. The energy gap between

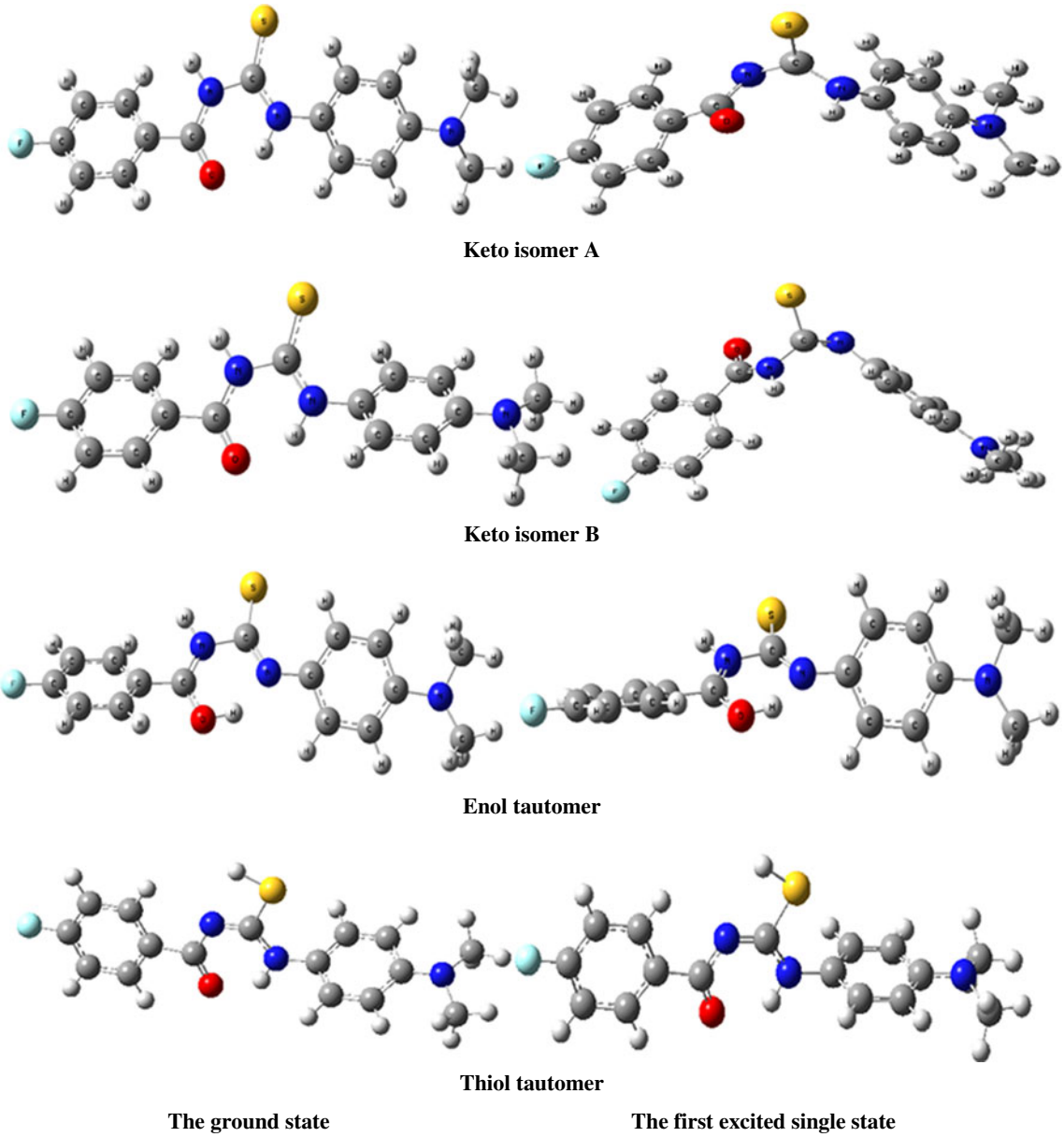

Fig. 7 Structures of the ground state and the first excited state of two tautomers and rotating isomers of 4FBDAPT

the lowest energy of S0 state corresponding to the minimum structures and the lowest energy of S1 state corresponding to the conformer of 90 ° is 2.48 eV. Comparing to the emission energy in THF 2.12 eV (584 nm), the error is 0.36 eV.

As we know, a charge-transfer transition should have a significant rearrangement of the electron density in the molecule. Frontier Molecular Orbitals (FMOs) obtained by MP2 method are shown in Fig. 9. The lowest energy transition involving exclusively HOMO→LUMO transition is suggested to be a charge-transfer state, which is characterized by transfer of electron density from toluidine ring to acylthiourea.

F3 fluorescence indicates the ESIPT characteristics. ESIPT is a phototautomerization in the excited state via an intramolecular hydrogen bond involving the transfer proton to the electronegative atom. It also indicates that a significant intramolecular relaxation takes place upon photo-excitation. The relaxation should increase the Stokes shift. F3 fluorescence bands have large Stokes shifts. The Stokes shift of 2FBDAPT of F3 band is 123 nm in THF, and 4FBDAPT of F3 band is 198 nm in THF. The fluorescence band shifts red as the polarity of the solvents increase. For example, the maximum wavelength of 4FBDAPT shifts from 459 nm in 1,4-dioxane to 472 nm in THF. And the fluorescence intensity enhances with the increase of the polarity of the solvents. The large BHWs of the fluorescence also indicate the ESIPT character. As we have known, the enol and thiol of these compounds exist stably by transfer one proton in the form of intramolecular hydrogen bond. If the relaxation of ESIPT undergoes the

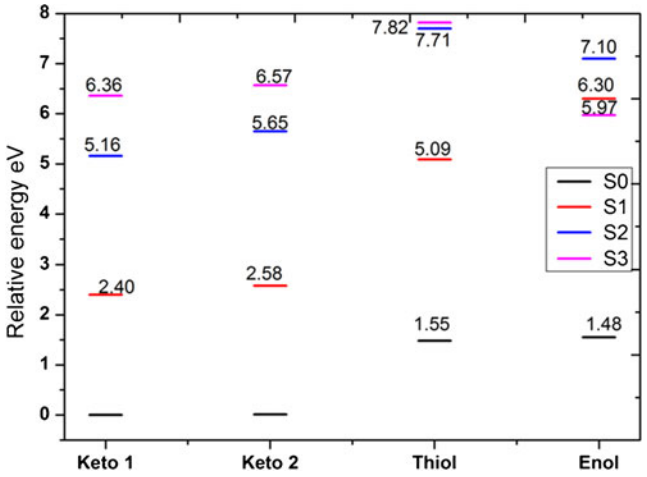

Fig. 8 Relative energy levels of tautomers and rotating isomers of 4FBDAPT

process by intramolecular proton transfer, from the CASSPT2 calculation, the energy gap of S1/S1' from the S1 state of thiol tautomer to the S1 state of keto tautomer is 2.69 eV and 2.51 eV, which is lower than the maximum emission energy, 2.70 eV (459 nm) in 1,4-dioxane of the fluorescence by 0.01 eV and 0.19 eV. Considering the larger error for the result of the enol tautomer, we attribute the fluorescence emission to the ESITP from the thiol tautomer to the keto tautomer. Considering the overestimation of CASSCF method for energy calculated of the transition [41], we suggest that the underestimation should result from the interaction between the title compounds and the solvent molecules.

The fluorescence at ca. 330 nm is proposed by Kasha to originate from the lowest energy singlet state, S1. But, we considered the F2 fluorescence band at 364 nm in 1,4-dioxane and 368 nm in acetonitrile of 4FBDAPT as the ESIPT fluorescence. Large Stokes shifts of 74 nm in dioxane and 110 nm in acetonitrile of the F2 band exhibit the existence of the relaxed geometric state, and the Stokes shifts increase as the polarity of the solvents increases. All of these indicate the ESIPT characteristic. The ESIPT should be taken place between the thiol and enol tautomers. The transition energy, $S1_T/S0_E$ from the first excited state of the thiol tautomer to the ground state of the enol tautomer is 3.61 eV. Comparing with the emission energy in fluorescence spectra, 3.4 eV (344 nm) in 1,4-dioxane, the error is 0.21 eV.

The intensity of the F1 fluorescence decreases quickly in the strong polar solvents. And the maximum of the fluorescence is almost independent of the solvent polarity. The fluorescence band should belong to LE fluorescence. We assign the F1 fluorescence band to the S1/S0 transitions of the enol tautomer. As shown in Fig. 8, there is no change on the structures between the first excited state and the ground state. That is to say, the first excited state belongs to Frank Condon state, and the transition from S1 to S0 can be a local transition. Normal Stokes shift of 50 nm displays the characteristic of LE. According to CASPT2 calculation, the energy gap between the first singlet excited state and the ground state is 4.49 eV. Comparing with the emission energy, 4.0 eV (310 nm) in 1,4-dioxane, the error is 0.49 eV.

Similar to common thiocarbonyls, the gap of S2→S1 of both keto isomers is larger than that of S1→S0. Strong S2-fluorescence is a common and regular feature in these kinds of compounds. The energy gap of the S2/S1 transition of both keto isomers is 2.76 eV and 3.03 eV respectively. The fluorescence emission energy of 2.70 eV in THF is slightly lower than the energy gap of S2/S1 of keto isomer, so we can't eliminate F3 fluorescence bands to S2/S1 of keto isomers. Similar to BA [22], the F4 fluorescence of TICT of both compounds annihilates in protic solvent, methanol.

Additionally, both F3 and F4 fluorescence in acetonitrile of 4FBDAPT shift blue unconventionally. The maxima emission wavelengths of F3 and F4 shift blue from 472 nm and 584 nm in THF to 463 nm and 550 nm in acetonitrile. The abnormal blue shifts are attributed to the intermolecular hydrogen bond interactions. The free proton of non-hydrogen bond in 4FBDAPT can form the intermolecular hydrogen bond with nitrogen atom of acetonitrile molecules of the solvent. According to the suggestion of Han et al. [42–44], comparing to the intermolecular hydrogen bond interaction of the ground state, which should decrease in the excited state, the weakening of hydrogen bond results in the blue shift of the fluorescence emission band.

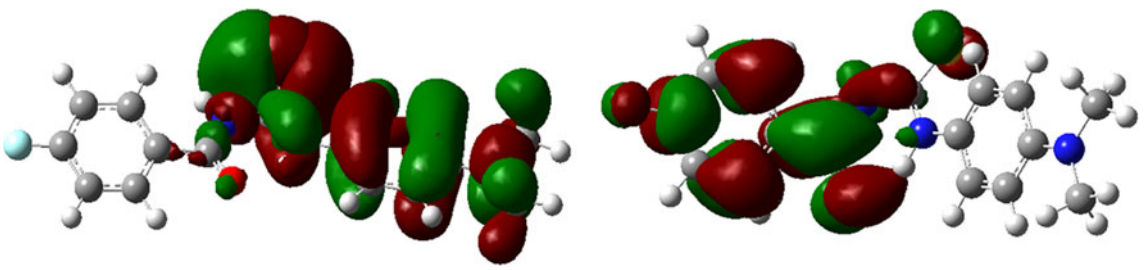

Fig. 9 Frontier Molecular Orbitals (FMOs) in the ground state by MP2 method

The formation of the intramolecular hydrogen bond interactions of N-H···F in the 2FBDAPT molecule reduced the dipolar moments of 2FBDAPT molecule. At the same time, it decreases the transition moments. The intensity of the fluorescence is lower than that of 4FBDAPT. The existence of the hydrogen bond of 2FBDAPT increases the coplanar of the 2FBDAPT. The twist from the most stable conformer to the conformer at 90 ° spends the more times. That is to say, the molecular relaxation time should increase, and the energy wastage in the deactivation of the excited state increases. Thus, the F4 fluorescence of TICT appears in the longer wavelength than that of 4FBDAPT. Additionally, for the structure of the excited state of the thiol tautomers (Fig. 8), both parts of benzoyl and thiol are almost the same planes, the proton transfer between the thiol tautomer and the good coplanar keto isomer of 2FBDAPT should be easier than that of 4FBDAPT. The energy wastage in the deactivation of the excited state should decrease. Therefore, Stokes shift of F3 in 2FBDAPT is smaller than that of in 4FBDAPT.

Conclusion

The attenuation of the long wave absorption bands in protic solvent is attributed to the intermolecular hydrogen bond interaction between the compounds and the solvent molecules. Quadruple fluorescence bands in studied solvents are observed. Similar to BA, F4 fluorescence emissions between 546 nm and 622 nm are assigned to TICT model and F3 emission bands from 434 nm to 483 nm are explained by the ESIPT model from the S1 state of the thiol tautomer to the S1 of the keto tautomer. Different from the fluorescence of BA, F2 emission bands are attributed to ESIPT from the S1 state of the thiol tautomer to the S0 state of the enol tautomer. F1 fluorescence emission originates from the local S1 transition of the enol tautomer. The fluorescence intensity of 2FBDAPT is weaker than that of 4FBDAPT, which results from the existence of the intramolecular hydrogen bond of N-H···F. The formation of the intermolecular hydrogen bond between a proton of non-hydrogen bond in 4FBDAPT and nitrogen atom of acetonitrile molecules of the solvent produces the blue shift of the charge transfer fluorescence of F4 and F3.

References

1. Beer PD, Gale PA (2001) Anion recognition and sensing: the state of the art and future perspectives. Angew Chem Int Ed 40:486–516
2. Kubo Y, Tsukahara M, Ishihara S, Tokita S (2000) A simple anion chemosensor based on a naphthalene–thiouronium dyad, Chem Commun 653–654
3. Fabbrizzi L, Leone A, Taglietti A (2001) A chemosensing ensemble for selective carbonate detection in water based on metal–ligand interactions. Angew Chem Int Ed 40:3066–3069
4. Wu FY, Jiang YB (2002) *p*-Dimethylaminobenzamide as an ICT dual fluorescent neutral receptor for anions under proton coupled electron transfer sensing mechanism. Chem Phys Lett 355:438–444
5. Wu JL, He YB, Zeng ZY, Wei LH, Meng LZ, Yang TX (2004) Synthesis of the anionic fluororeceptors based on thiourea and amide groups and recognition property for α, ω-dicarboxylate. Tetrahedron 60:4309–4314
6. Rodríguez L, Alves S, Lima JC, Parola AJ, Pina F, Sorianoc C, Albelda T, García-España E (2003) Supramolecular interactions of hexacyanocobaltate(III) with polyamine receptors containing a terminal anthracene sensor. J Photoch Photobiol A 159:253–258
7. Hennrich G, Sonnenschein H, Resch-Genger U (2001) Fluorescent anion receptors with iminoylthiourea binding sites—selective hydrogen bond mediated recognition of CO_3^{2-}, HCO_3^{-} and HPO_4^{2-}. Tetrahedron Lett 42:2805–2808
8. Zhang XA, Woggon WD (2005) A supramolecular fluorescence sensor for pyrovanadate as a functional model of vanadium haloperoxidase. J Am Chem Soc 127:14138–14139
9. Blanco JLJ, Bootello P, Benito JM, Mellet CO, Fernández JMG (2006) Urea-, thiourea-, and guanidine-linked glycooligomers as phosphate binders in water. J Org Chem 71:5136–5143
10. Nie L, Li Z, Han J, Zhang X, Yang R, Liu WX, Wu FY, Xie JW, Zhao YF, Jiang YB (2004) Development of *N*-Benzamidothioureas as a new generation of thiourea-based receptors for anion recognition and sensing. J Org Chem 69:6449–6454
11. Wu FY, Hu MH, Wu YM, Tan XF, Zhao YQ, Ji ZJ (2006) Fluoride-selective colorimetric sensor based on thiourea binding site and anthraquinone reporter. Spectrochim Acta A 65:633–637
12. Martinez-Máñez R, Sancenón F (2006) Chemodosimeters and 3D inorganic functionalised hosts for the fluoro-chromogenic sensing of anions. Coordin Chem Rev 250:3081–3093
13. Wu FY, Ma LH, Jiang YB (2001) Fluorescence sensing of anions based on a novel dual fluorescentneutral receptor N-(4-dimethylamionbenzoyl)thiourea. Anal Sci 17(Supplement):i801–i803
14. Wu FY, Li Z, Guo L, Wang X, Lin MH, Zhao YF, Jiang YB (2006) A unique NH-spacer for N-benzamidothiourea based anion sensors. Substituent effect on anion sensing of the ICT dual fluorescent N-(p-dimethylaminobenzamido)-N-arylthioureas. Org Biomol Chem 4:624–630
15. Li HB, Yan HJ (2009) Ratiometric fluorescent mercuric sensor based on thiourea-thiadiazole-pyridine linked organic nanoparticles. J Phys Chem C 113:7526–7530
16. Heldt J, Gormin D, Kasha M (1988) The triple fluorescence of benzanilide and the dielectric medium modulation of its competitive excitation. Chem Phys Lett 150:433–436
17. Heldt J, Gormin D, Kasha M (1988) Intramolecular charge-transfer transition in benzanilides and its dielectric medium modulation. J Am Chem Soc 110:8255–8256
18. Heldt J, Gormin D, Kasha M (1989) A comparative picosecond spectroscopic study of the competitive triple fluorescence of aminosalicylates and benzanilides. Chem Phys 136:321–334
19. Azumaya I, Kagechika H, Fujiwara Y, Itoh M, Yamaguchi K, Shudo K (1991) Twisted intramolecular charge-transfer fluorescence of aromatic amides: conformation of the amide bonds in excited states. J Am Chem Soc 113:2833–2838
20. O'Connell EJ, Delmauro M, Irwin J (1971) Absorption and emission studies of electronic states of N-arylbenzamides. Photochem Photobiol 14:189–195
21. Tang GQ, MacInnis J, Kasha M (1987) Proton-transfer spectroscopy of benzanilide. Amide-imidol tautomerism. J Am Chem Soc 109:2531–2533
22. Lewis FD, Long TM (1998) Anomalous dual fluorescence of benzanilide. J Phys Chem A 102:5327–5332
23. Yang W, Zhou WQ, Zhang ZJ (2007) Structural and spectroscopic study on *N*-2-fluorobenzoyl-*N*′-4-methoxyphenylthiourea. J Mol Struct 828:46–53

24. Altomare A, Burla M, Camalli M, Cascarano G, Giacovazzo C, Guagliardi A, Moliterni A, Polidori G, Spagna R (1999) SIR97: a new tool for crystal structure determination and refinement. J Appl Cryst 32:115–119
25. Beurskens PT, Admiraal G, Beurskens G, Bosman WP, de Gelder R, Israel R, Smits JMM (1999) The DIRFID-99 Program System, Technical Report of the Crystallography Laboratory. University of Nijmegen, Nijmegen, The Netherlands
26. Zwier TS (1996) The spectroscopy of solvation in hydrogen-bonded aromatic clusters. Annu Rev Phys Chem 47:205–241
27. Southern A, Levy DH, Florio GM, Longarte A, Zwier TS (2003) Electronic and infrared spectroscopy of anthranilic acid in a supersonic jet. J Phys Chem A 107:4032–4040
28. Clarkson JR, Baquero E, Shubert VA, Myshakin EM, Jordan KD, Zwier TS (2005) Laser-initiated shuttling of a water molecule between H-bonding sites. Science 307:1443–1446
29. Frisch MJ, Trucks GW, Schlegel HB, Scuseria GE, Robb MA, Cheeseman JR, Scalmani G, Barone V, Mennucci B, Petersson GA, Nakatsuji H, Caricato M, Li X, Hratchian HP, Izmaylov AF, Bloino J, Zheng G, Sonnenberg JL, Hada M, Ehara M, Toyota K, Fukuda R, Hasegawa J, Ishida M, Nakajima T, Honda Y, Kitao O, Nakai H, Vreven T, Montgomery JA Jr, Peralta JE, Ogliaro F, Bearpark M, Heyd JJ, Brothers E, Kudin KN, Staroverov VN, Kobayashi R, Normand J, Raghavachari K, Rendell A, Burant JC, Iyengar SS, Tomasi J, Cossi M, Rega N, Millam JM, Klene M, Knox JE, Cross JB, Bakken V, Adamo C, Jaramillo J, Gomperts R, Stratmann RE, Yazyev O, Austin AJ, Cammi R, Pomelli C, Ochterski JW, Martin RL, Morokuma K, Zakrzewski VG, Voth GA, Salvador P, Dannenberg JJ, Dapprich S, Daniels AD, Farkas Ö, Foresman JB, Ortiz JV, Cioslowski J, Fox DJ (2009) Gaussian 09. Gaussian, Inc., Wallingford CT
30. El Azhary A, Rauhut G, Pulay P, Werner HJ (1998) Analytical energy gradients for local second-order Møller–Plesset perturbation theory. J Chem Phys 108:5185–5193
31. Werner HJ, Knowles PJ (1985) A second order multiconfiguration SCF procedure with optimum convergence. J Chem Phys 82:5053–5063
32. Knowles PJ, Werner HJ (1985) An efficient second-order MC SCF method for long configuration expansions. Chem Phys Lett 115:259–267
33. Werner HJ (1996) Third-order multireference perturbation theory The CASPT3 method. Mol Phys 89:645–661
34. Celani P, Werner HJ (2000) Multireference perturbation theory for large restricted and selected active space reference wave functions. J Chem Phys 112:5546–5557
35. Werner HJ, Knowles PJ, Lindh R, Manby FR, Schütz M, Celani P, Korona T, Mitrushenkov A, Rauhut G, Adler TB, Amos RD, Bernhardsson A, Berning A, Cooper DL, Deegan MJO, Dobbyn AJ, Eckert F, Goll E, Hampel C, Hetzer G, Hrenar T, Knizia G, Köppl C, Liu Y, Lloyd AW, Mata RA, May AJ, McNicholas SJ, Meyer W, Mura ME, Nicklass A, Palmieri P, Pflüger K, Pitzer R, Reiher M, Schumann U, Stoll H, Stone AJ, Tarroni R, Thorsteinsson T, Wang M, Wolf A, *MOLPRO*, version 2008.1
36. Maciejewski A, Steer RP (1993) The photophysics, physical photochemistry, and related spectroscopy of thiocarbonyls. Chem Rev 93:67–98
37. Szymanski M, Maciejewski A, Steer RP (1988) Radiationless decay of aromatic thiones in solution selectively excited to their S3, S2, S1, and T1 states. J Phys Chem 92:2485–2489
38. Lippert E, Lflder W, Boos H in: Advances in Molecular Spectroscopy, 1962, ed. A. Mangini (Pergamon Press, Oxford), 443
39. Rettig W (1986) Ladungstrennung in angeregten Zuständen entkoppelter Systeme – TICT-Verbindungen und Implikationen für die Entwicklung neuer Laserfarbstoffe sowie für den Primärprozeß von Sehvorgang und Photosynthese. Angew Chem 98:969–986
40. Albrecht M, Bohne C, Granzhan A, Ihmels H, Pace TCS, Schnurpfeil A, Waidelich M, Yihwa C (2007) Dual fluorescence of 2-methoxyanthracene derivatives. J Phys Chem A 111:1036–1044
41. Han KL, Zhao GJ (2010) Hydrogen bonding and transfer in the excited state. John Wiley & Sons Ltd, UK
42. Zhao GJ, Han KL (2008) Effects of hydrogen bonding on tuning photochemistry: concerted hydrogen-bond strengthening and weakening. Chem Phys Chem 9:1842–1846
43. Zhao GJ, Han KL (2009) Role of intramolecular and intermolecular hydrogen bonding in both singlet and triplet excited states of aminofluorenones on internal conversion, intersystem crossing, and twisted intramolecular charge transfer. J Phys Chem A 113:14329–14335
44. Zhao GJ, Han KL (2010) pH-Controlled twisted intramolecular charge transfer (TICT) excited state *via* changing the charge transfer direction. Phys Chem Phys Chem 12:8914–8918